EARTH SURFACE PROCESSES AND LANDFORMS
Earth Surf. Process. Landforms **43**, 2926–2934 (2018)

Published online 24 July 2018 in Wiley Online Library
(wileyonlinelibrary.com) DOI: 10.1002/esp.4460

Sheet erosion rates and erosion control on steep rangelands in loess regions

Dongdong Wang,[1] Zhanli Wang,[1,2*] Qingwei Zhang,[1] Qilin Zhang,[1] Naling Tian[1] and Jun'e Liu[3,4]

[1] State Key Laboratory of Soil Erosion and Dryland Farming on the Loess Plateau, Institute of Soil and Water Conservation, Northwest A&F University, Yangling, Shaanxi 712100, China
[2] Institute of Soil and Water Conservation, Chinese Academy of Sciences and Ministry of Water Resources, Yangling, Shaanxi 712100, China
[3] School of Geography and Tourism, Shaanxi Normal University, Xi'an, Shaanxi 710119, China
[4] National Demonstration Center for Experimental Geography Education, Shaanxi Normal University, Xi'an, Shaanxi 710119, China

Received 3 May 2017; Revised 7 June 2018; Accepted 18 June 2018

*Correspondence to: Zhanli Wang, State Key Laboratory of Soil Erosion and Dryland Farming on the Loess Plateau, Institute of Soil and Water Conservation, Northwest A&F University, Yangling, Shaanxi 712100, China. E-mail: zwang@nwsuaf.edu.cn

ESPL
Earth Surface Processes and Landforms

ABSTRACT: Numerous steep rangelands have been restored from abandoned steep croplands, and sheet erosion has become the dominant erosion process on rangelands since the Grain-to-Green Project was launched in 1999 on the Loess Plateau. Quantifying sheet erosion rates and dynamics on steep rangelands may aid soil erosion management strategies and improve grassland health. Simulated rainfall experiments were conducted on a rangeland plot under five vegetation coverages (30%, 40%, 50%, 60% and 70%), five rainfall intensities (0.7, 1.0, 1.5, 2.0 and 2.5 mm min^{-1}) and five slopes (7°, 10°, 15°, 20° and 25°). The results show that the sheet erosion rate decreased as vegetation cover increased, as described by linear or logarithmic equations under different rainfall intensities or slopes. Herbaceous vegetation can reduce and control sheet erosion by reducing the effect of rainfall intensity or slope, especially under sufficiently high vegetation cover. The sheet erosion rate was accurately modelled by a linear equation that included the three factors, i.e. rainfall intensity, vegetation cover, and slope. Among the different hydrodynamic parameters (shear stress, stream power, unit stream power and unit energy), stream power resulted in the best model for the sheet erosion rate. Velocity measurements and calculations, water depth calculations, and aggregative indicators of herbaceous vegetation for sheet flow should be explored in future research, which will be important in improving experimental accuracy and sheet erosion modelling. © 2018 John Wiley & Sons, Ltd.

KEYWORDS: sheet erosion rate; erosion control; steep rangelands; loess region; hydraulic parameters

Introduction

The Loess Plateau is one of the most severe soil erosion regions in the world. Since the Grain-to-Green Project, which restores cropland to forest land or rangeland for the purpose of controlling soil erosion, was launched in 1999 on the Loess Plateau, numerous steep rangelands have been restored from abandoned steep croplands, and sheet erosion has become the dominant erosion process on rangelands (Wei *et al*. 2009; Nearing *et al*. 2011). Quantification of sheet erosion rates and dynamics on steep rangelands by studying sheet erosion rates and erosion control on these rangelands in loess regions can significantly aid soil erosion management strategies and improve grassland health.

Through the action of raindrops and shallow running water, sheet erosion induces the uniform removal of a thin layer or 'sheet' of the fertile upper soil horizon (Dlamini *et al*. 2011). This phenomenon is now recognized as a major threat to the sustainability of natural ecosystems (Wight and Lovely 1982; UNEP 1994). In addition, from a global perspective, rangelands cover approximately 50% of the Earth's land surface (Williams *et al*. 1968; Prentice *et al*. 1992) and are characteristically located in arid and semi-arid climates; the importance of preventing soil erosion in these climates has long been recognized (Carroll *et al*. 1997; Morgan 2005; Wei *et al*. 2007). Therefore, modelling the sheet erosion rate on rangelands is vital for evaluating and maintaining grassland health (Pyke *et al*. 2002; Pellant *et al*. 2005). Moreover, modelling the sheet erosion rate on steep rangelands restored from abandoned croplands can extend the knowledge of sheet erosion in these regions and can provide useful references for evaluating and maintaining grassland health, in addition to facilitating soil conservation and ecological construction on the Loess Plateau.

Rangeland erosion has been studied extensively. For example, in 1983/1984, research was conducted to identify methods to assess grazing lands on the commons of the East-Húnavatnssýsla district in Iceland (Aradottir and Arnalds 1985). The Icelandic Science Foundation funded some general research on soil erosion to determine different types of erosion (Arnalds *et al*. 2001). Predicted high-erosion zones agreed well with the long-term patterns of erosion and deposition in a catchment located in Wagga, Australia (Moore and Burch,

1986). There was a significant negative relationship between the final runoff rate and plant cover, and plant cover had no significant effect on sediment concentration in a semi-arid wooded rangeland in eastern Australia (Greene *et al*. 1994; Oudenhoven *et al*., 2015). Rainfall simulation studies on rangeland in the Ntondozi area of Swaziland showed that soil loss decreased exponentially with increasing vegetation cover (Morgan *et al*. 1997). Vegetation exerts considerable hydrological control by increasing the infiltration capacity of soil, which consequently influences the timing and duration of runoff (Morgan *et al*. 1997).

Erosion models are effective tools for soil erosion prediction and management strategies, which usually require the use of hydraulic parameters. For example, the water erosion prediction project (WEPP) (Nearing *et al*. 1989) used shear stress, the European soil erosion model (EUROSEM) (Morgan 1995) and the Limburg soil erosion model (LISEM) (De Roo *et al*. 1996) used unit stream power, while the Griffith university erosion system template (GUEST) (Misra and Rose, 1996) used stream power. Fox and Bryan (2000) and Fan and Wu (1999) suggested that the sheet erosion rate could be estimated using a linear function of unit stream power, which could predict the sheet erosion rate better than shear stress. Cao *et al*. (2015) determined that soil loss on a loess road surface could be estimated using a linear function of stream power, and their findings agreed with those of Huang (1995).

Process descriptions in physically based models, such as water erosion prediction project (WEPP) (Flanagan and Nearing, 1995) and rangeland hydrology and erosion model (RHEM) (Nearing *et al*. 2011), are complex. An erosion model to predict soil loss specific to rangeland applications is needed because existing erosion models, such as WEPP, were developed from croplands that have different hydrologic and erosion processes (Nearing *et al*. 2011). A new splash and sheet erosion equation specific to rangelands was developed based on the rangeland database (Wei *et al*. 2009). In addition, model sensitivity and uncertainty analyses were conducted (Wei *et al*. 2007; 2008). RHEM estimates runoff, erosion, and sediment delivery rates and volumes at the spatial scale of a hillslope and the temporal scale of a single rainfall event to provide reasonable runoff and soil loss prediction capacities for rangeland management (Nearing *et al*. 2011).

While research into sheet erosion on rangelands has been conducted (Wei *et al*. 2007; 2008;2009 ; Nearing *et al*. 2011), this is not the case for steep rangelands restored from abandoned croplands in loess regions.

The experiments in this study were conducted on steep rangelands restored from abandoned croplands in the loess region. The following objectives were established: (1) to identify variations in the sheet erosion rate on rangelands with different levels of herbaceous vegetation cover under different rainfall intensities and slopes; and (2) to model the sheet erosion rate on rangelands in response to three factors, i.e. rainfall intensity, slope, and herbaceous vegetation cover, to reveal the sheet erosion characteristics and to model the sheet erosion rate on rangelands as a function of hydraulic parameters (shear stress, stream power, unit stream power, and unit energy) to clarify the dynamic mechanism of sheet erosion.

Materials and methods

Test locations and soil

Experiments were conducted in the Simulated Rainfall Hall of the State Key Laboratory of Soil Erosion and Dryland Farming on the Loess Plateau at the Institute of Soil and Water Conservation, Chinese Academy of Science and Ministry of Water Resources. The soil samples for testing were obtained from Ansai County in the hinterland of the Loess Plateau (a typical region with hills and gullies). Ansai (109°19′ E, 36°51′ N) is in northern Shaanxi Province of China and has a mean annual temperature of 8.8°C and mean annual precipitation of 500 mm. The soil samples were air-dried and subsequently sieved through a 5 mm mesh to remove stones, grass, and other debris. The soil samples were then wetted by light spraying to achieve a soil water content of 14%. The soil contained 70.09% sand (0.02–2.0 mm), 21.42% silt (0.002–0.02 mm) and 8.49% clay (<0.002 mm). The average diameter of the test soil particles was 0.039 mm.

Rangeland plot and experimental design

Metal-framed soil pans (80 cm long, 60 cm wide, and 25 cm deep) were used to make rangeland plots; grass was transplanted into the pans that were filled with soil. The slope gradient of the plot could be adjusted between 0% and 84% using the movable base of the plot frame. An outlet at the lower end of each plot frame allowed the collection of runoff samples. At the bottom of each plot, 5 cm of natural sand was overlaid with permeable gauze to allow drainage of infiltrated water. The soil in the plot was packed to a depth of 20 cm in four 5-cm layers with a smooth soil surface, i.e. the microtopography did not fluctuate, at a bulk density of 1.2 g/cm^3 (measured using compacted soil and sampled by a cutting ring). Before the soil was packed in the plot, the soil water content was adjusted to 14%, which is the typical level on the Loess Plateau during the flood season when maximum erosion occurs (Liu *et al*. 2014). After the soil was packed, herbaceous vegetation (*Poa pratensis* L.) was transplanted into the plot in a banded uniform layout. The rangeland plot for the simulated rainfall experiment was then completely formed. *Poa pratensis* L. is a gramineous plant, and current-year grass was selected for the experiments. The simulated rainfall experiments were initiated approximately 2 months after planting, when the vegetation exhibited stable growth in the rangeland plot and the soil surface was no longer disturbed. A complementary border area with a width of 27.5 cm was established around the plot, i.e. the test area. The border area was filled with soil, and grass was transplanted in the same manner as in the plot to ensure equal splashing onto and off the plot such that erosion in the plot closely resembled that in the field. The vegetation cover, expressed as a percentage, was determined using digital images that were processed using ImageJ software (National Institutes of Health, Bethesda, Maryland, United States) before the simulated rainfall was initiated.

Five levels of herbaceous vegetation cover, i.e. grass canopy cover (30%, 40%, 50%, 60%, and 70%), five rainfall intensities (0.7, 1.0, 1.5, 2.0, and 2.5 mm min^{-1}) and five slopes (7°, 10°, 15°, 20°, and 25°) were tested in one replicate per run; a total of 90 experimental events were simulated (Table I). The duration of all simulated rainfall events was 40 min. The raindrop kinetic energies of the various rainfall intensities (0.7, 1.0, 1.5, 2.0, and 2.5 mm min^{-1}) were 193.87, 274.41, 380.06, 506.94, and 704.75 J s^{-1} m^{-2}, respectively.

Measurements

In each treatment, runoff samples were collected 1 min and 3 min after the onset of runoff and then every 3 min until the end of the experiment. The mass of each runoff sample was measured using a scale, and the samples were maintained at 105°C to evaporate the water and to dry the sediment.

Table I. Experiment design

Slope (°)	Rainfall intensity (mm min^{-1})	Cover (%)	Repeat	Event
15	0.7, 1.0, 1.5, 2.0, 2.5	30, 40, 50, 60, 70	1	50
7, 10, 15, 20, 25	1.5	30, 40, 50, 60, 70	1	50
Remark	10 events were repeated			
Total				90

Sediment samples were weighed once, when dry. The velocity of the flow surface was determined using $KMnO_4$ as a tracer, and velocity measurements were replicated once. The mean sheet flow depth (m) of the slope surface of the plot was calculated by dividing the flow discharge per unit width (m^2 s^{-1}) by the average velocity (m s^{-1}) of two measurements. The water temperature was monitored using a thermometer. The runoff rate (m s^{-1}) was defined as runoff volume per unit projected area per unit time (m^3 m^{-2} s^{-1}), whereas the erosion rate (kg m^{-2} s^{-1}) was defined as sediment mass per unit projected area per unit time. The mean sheet erosion was calculated by averaging all sheet erosion rates of individual rainfall events for each combination of slope, vegetation cover, and rainfall intensity. The Reynolds number (Re) was calculated for each case in which runoff occurred to determine the flow regime of runoff; the mean flow velocity of the runoff layer was obtained by multiplying the runoff surface velocity by 0.67 (Horton *et al*. 1934).

Hydraulic parameters

Shear stress (τ, measured in Pa; Nearing *et al*. 1991), stream power (ω, measured in W m^{-2}; Bagnold 1966; Prosser and Rustomji 2000), and unit stream power (U, measured in m s^{-1}; Yang 1972, 1976) were calculated as follows:

$$\tau = \rho g \mathrm{h} S \tag{1}$$

where ρ is the density of water (kg m^{-3}), g is gravitational acceleration (m s^{-2}), h is the flow depth (m), and S is the sine value of the slope gradients;

$$\omega = \tau V = \rho g h S V \tag{2}$$

where V is the mean flow velocity (m s^{-1}); and.

$$U = VS \tag{3}$$

the unit energy (E, measured in cm; Zhao and He 2010) was calculated as

$$E = \alpha V^2 (2g)^{-1} + h\cos\theta \tag{4}$$

where α is the kinetic energy correction factor (α= 1), and θ is the slope angle (°).

Data analysis

All statistical analyses were performed using Microsoft Excel. The dataset (n = 45) was used for modelling the sheet erosion rate, describing the influence of herbaceous vegetation on the sheet erosion rate and deriving the values of the statistical parameter R^2. The modelling results were evaluated using independently measured data (Table II). The dataset (n=16) of the independently measured data was used for equation validation by generating the value of the statistical parameter Nash–Sutcliffe efficiency index (NE), which is used to evaluate the performance of modelling equations. The following statistical parameters were used to evaluate the performance of the simulated results:

$$NE = 1 - \frac{\sum (O_i - P_i)^2}{\sum \left(O_i - \overline{O}\right)^2} \tag{5}$$

where NE is the Nash–Sutcliffe efficiency index (Nash and Sutcliffe 1970), O_i is the measured value, P_i is the predicted value, $\overline{O}$ is the average measured value.

Results

Effect of herbaceous vegetation on the sheet erosion rate

Variation in the sheet erosion rate with different herbaceous vegetation coverages under different rainfall intensities or slopes

The sheet erosion rate decreases with increase in cover under different rainfall intensities or slopes, as shown in Figure 1; this change is well described by linear equations or logarithmic equations (Table III). The extent of the decrease is initially low and then increases and is maximized under 30–40% and 60–70% cover (Figure 1). Therefore, herbaceous vegetation can reduce sheet erosion, and sufficiently high vegetation cover can control sheet erosion.

Variation in the sheet erosion rate with rainfall intensities or slopes under different herbaceous vegetation coverages

The sheet erosion rate increases with rainfall intensity or slope under the same cover, as shown in Figure 2; this increase can be described by power equations (Table IV). The extent of the increase is initially high and then decreases (Figure 2). Therefore, herbaceous vegetation can reduce the effect of high rainfall intensity or slope on sheet erosion.

Modelling the sheet erosion rate using rainfall intensity, slope, and cover

The sheet erosion rate increases with increase in the slope or rainfall intensity and a decrease in the vegetation cover. A comparison between the observed and modelled sheet erosion rate

Table II. Conditions of independent measured data

Slope (°)	Rainfall intensity (mm min^{-1})	Cover (%)	Repeat	Event
7	0.7, 2.5	30, 60	0	4
10	1.0, 2.0	40, 50	0	4
20	0.7, 2.0	30, 70	0	4
25	1.0, 2.5	40, 60	0	4
Total				16

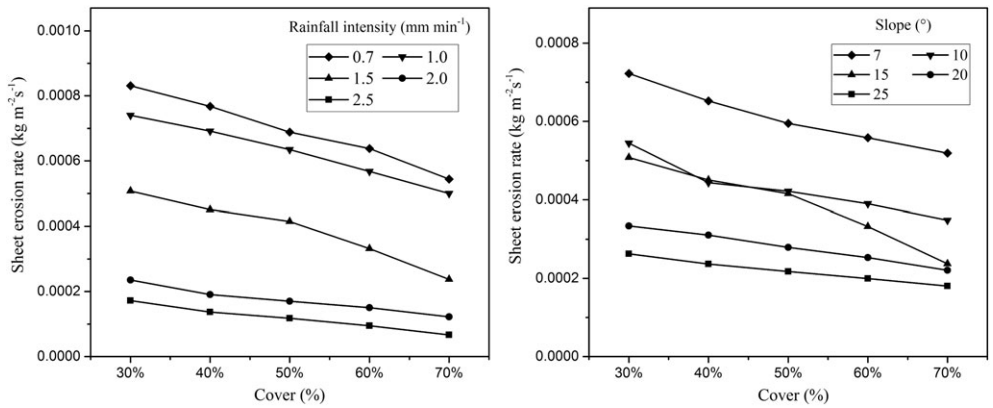

Figure 1. Variations of sheet erosion rate (SE) with cover under different rainfall intensities or slopes.

Table III. Relationship of sheet erosion rate and cover under different rainfall intensities or slopes

Rainfall intensity (mm min^{-1})	Empirical equation	R^2	Slope (°)	Empirical equation	R^2	P
0.7	SE = -0.0003C +0.0002	0.991	7	SE = -0.0002ln(C) + 0.0004	0.996	0.01
1.0	SE = -0.0003C +0.0003	0.973	10	SE = -0.0002ln(C) + 0.0003	0.973	0.01
1.5	SE = -0.0007C +0.0007	0.970	15	SE = -0.0003ln(C) + 0.0002	0.920	0.01
2.0	SE = -0.0006C +0.0009	0.995	20	SE = -0.000ln(C) + 0.0004	0.958	0.01
2.5	SE = -0.0007C +0.001	0.993	25	SE = -0.000ln(C) + 0.0005	0.999	0.01

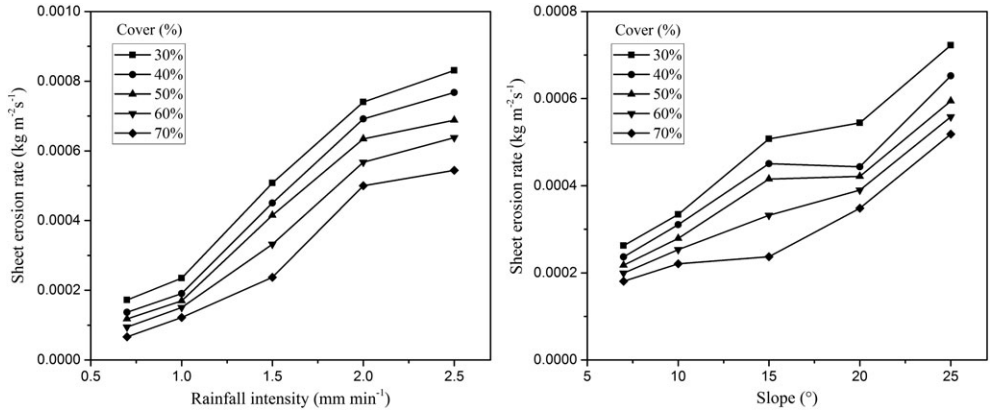

Figure 2. Variations of sheet erosion rate (SE) with rainfall intensity or slope under different covers.

Table IV. Relationship of sheet erosion rate and rainfall intensity or slope under different covers

Cover (%)	Empirical equation	R^2	Empirical equation	R^2	P
30	SE= $0.0003I^{1.13426}$	0.977	SE = $6E\text{-}05S^{0.7765}$	0.979	0.01
40	SE= $0.0002I^{1.14809}$	0.974	SE = $6E\text{-}05S^{0.7316}$	0.994	0.01
50	SE= $0.0002I^{1.1521}$	0.971	SE = $5E\text{-}05S^{0.7462}$	0.961	0.01
60	SE= $0.0002I^{1.16038}$	0.960	SE = $4E\text{-}05S^{0.7563}$	0.968	0.01
70	SE= $0.0001I^{1.1744}$	0.984	SE = $4E\text{-}05S^{0.7614}$	0.783	0.01

(SE) indicates that SE can be modelled by a power function that includes rainfall intensity and vegetation cover (Figure 3), by a power function that includes slope and vegetation cover (Figure 4), and by a linear equation that includes rainfall intensity, vegetation cover or slope (Figure 5), expressed as follows:

$$SE = 0.00011\ C^{-0.708}\ I^{1.538}\ R^2 = 0.97, NE = 0.72, \quad (6)$$

$$SE = 0.00003\ C^{-0.524}\ S^{0.754}\ R^2 = 0.96, NE = 0.12, \quad (7)$$

$$SE = -0.00023 - 0.00044C + 0.00035I + 0.00002S\ R^2 = 0.96, NE = 0.85, \quad (8)$$

where SE is the sheet erosion rate (kg m^{-2} s^{-1}); S is the slope (°); I is the rainfall intensity (mm·min^{-1}); and C is vegetation cover (%). Equation (8) shows that the absolute value of the equation coefficient is C (0.00044) > I (0.00035) > S (0.00002), which shows that the relative ranking of the three factors that influence sheet erosion is C > I > S. NE shows that the SE can be adequately modelled by a linear equation that includes vegetation cover, rainfall intensity and slope or by a power function that includes rainfall intensity and vegetation cover. However, modelling SE using vegetation cover and slope yields poor results.

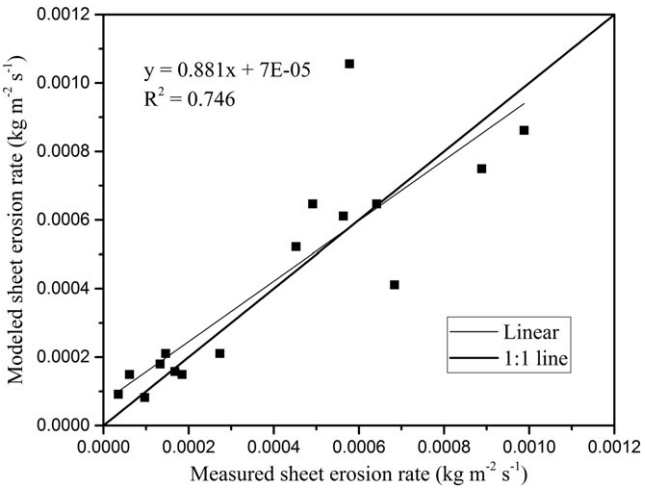

Figure 3. Measured versus modelled sheet erosion rate (SE) ($SE=0.00011\ C^{-0.708}\ I^{1.538}$).

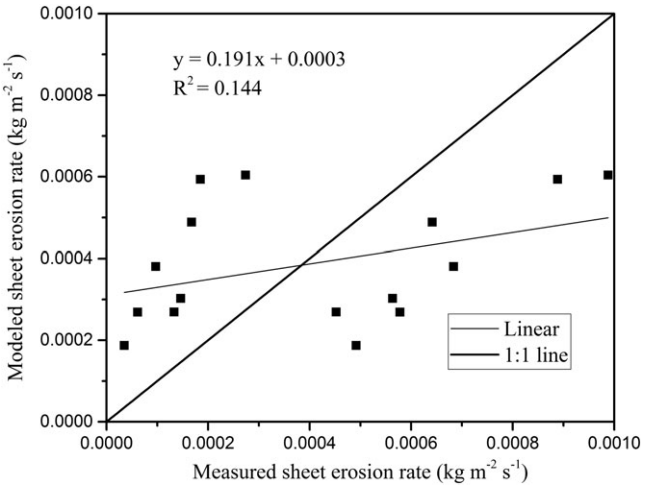

Figure 4. Measured versus modelled sheet erosion rate (SE) ($SE=0.00003\ C^{-0.524}\ S^{0.754}$).

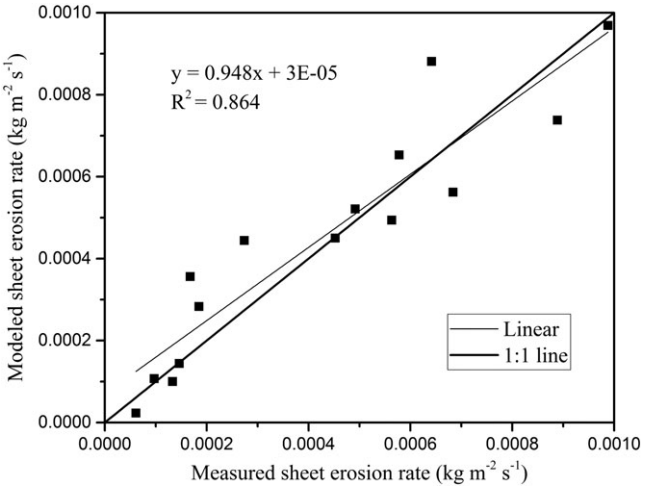

Figure 5. Measured versus modelled sheet erosion rate (SE) (SE= -0.00023-0.00044C. + 0.00035I+0.00002S).

Modelling SE using hydraulic parameters

Shear stress

SE increases with shear stress for all combinations of rainfall intensity, vegetation cover, and slope, and the relationship can be defined by a power function (Figure 6). A comparison between the observed and predicted SE (Figure 7) indicates that SE can be modelled by a power function that includes shear stress, expressed as:

$$SE = 0.0029\tau^{1.601}\ R^2 = 0.79, NE = 0.55, \quad (9)$$

Equation (9) shows that the soil erodibility parameter is 0.0029 s m^{-1}, NE is 0.55, and R^2 is 0.79. NE shows that SE for all combinations of rainfall intensity, vegetation cover, and slope can be modelled by a power function that includes shear stress.

Stream power

SE increases with stream power for all combinations of rainfall intensity, vegetation cover, and slope; the relationship can be fitted with a simple linear equation (Figure 6), which is expressed in Equation (10). A comparison between the observed and modelled SE indicates good agreement (Figure 8).

$$SE = 0.0154\ (\omega - 0.00325)\ R^2 = 0.93, NE = 0.89 \quad (10)$$

Equation (10) shows that the soil erodibility parameter is 0.0154 $s^2\ m^{-2}$, the critical stream power is 0.00325 W m^{-2}, NE is 0.89, and R^2 is 0.93. NE shows that SE under different rainfall intensities, vegetation coverages, and slopes can be adequately modelled by a linear equation that includes stream power.

Unit stream power

SE increases as unit stream power increases; the relationship for all combinations of rainfall intensity, vegetation cover, and slope can be described by a linear equation (Figure 6), which is expressed in Equation (11). A comparison between the observed and predicted SE shows poor agreement (Figure 9).

$$SE = 0.0148\ (U - 0.0003)\ R^2 = 0.60, NE = 0.31, \quad (11)$$

Equation (11) shows that the critical unit stream power is 0.0003 m s^{-1}, the soil erodibility parameter is 0.0148 kg m^{-3}, NE is 0.31, and R^2 is 0.60. NE indicates that SE in this study cannot be modelled by a linear unit stream equation.

Unit energy

The relationship between SE and unit energy for all combinations of rainfall intensity, vegetation cover, and slope can be fitted with a linear equation (Figure 6), which is expressed in Equation (12). A comparison of the observed and modelled SE shows good agreement (Figure 10), expressed as follows:

$$SE = 0.0090\ (E - 0.0212)\ R^2 = 0.85, NE = 0.79, \quad (12)$$

Equation (12) shows that the critical unit energy is 0.0212 cm, the soil erodibility parameter is 0.009 kg $m^{-3}\ s^{-1}$, NE is 0.79, and R^2 is 0.85. NE indicates that SE in this study is adequately modelled by a linear unit energy equation.

Discussion

Herbaceous vegetation reduces sheet erosion on rangeland

Herbaceous vegetation effectively reduces sheet erosion by decreasing the effect of rainfall intensity or slope, and sheet erosion can be controlled by sufficiently high vegetation cover (Figure 1). Moreover, SE can be adequately modelled by a

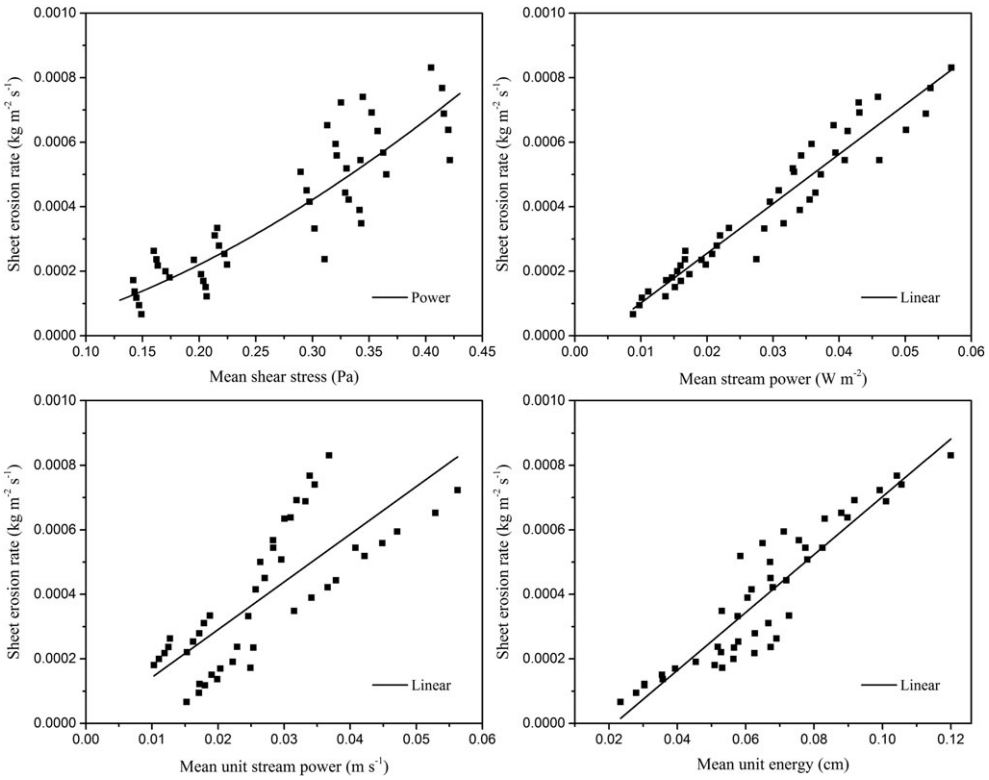

Figure 6. Relationship between sheet erosion rate (SE) and hydraulic parameters at all combinations of rainfall intensities, vegetation covers and slopes.

linear equation that includes rainfall intensity, vegetation cover, and slope, which is different from the relationship between sheet erosion and rainfall intensity on bare slopes (Meyer 1981).

Sheet erosion is produced by the combined power of raindrop-impacted sheet flow and the resistance of soil to this flow. Herbaceous vegetation can decrease the power of raindrop-impacted sheet flow by increasing infiltration and by decreasing the runoff amount, turbulence and velocity. Herbaceous vegetation can also increase soil resistance to raindrop-impacted sheet flow as follows: the detachment of soil particles from the soil parent body is decreased because vegetation intercepts raindrops that would otherwise directly impact the soil surface, and soil stability is increased through the vegetation root system. Consequently, herbaceous vegetation can greatly reduce SE on rangelands.

A comparison of the modelling result using Equation (8) and that using RHEM (Wei *et al*. 2009; Nearing *et al*. 2011) shows that Equation (8) with NE = 0.85 is better than RHEM with NE = 0.59 when modelling SE under certain conditions.

Modelling SE on rangeland using hydraulic parameters

Sheet flow produces sheet erosion, and the flow power can be expressed by different hydraulic parameters.

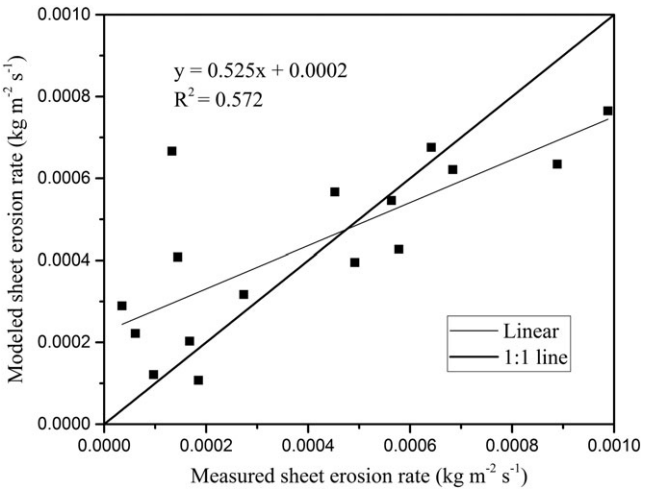

Figure 7. Measured versus modelled sheet erosion rate (SE) (SE= $0.0029\tau^{1.601}$)).

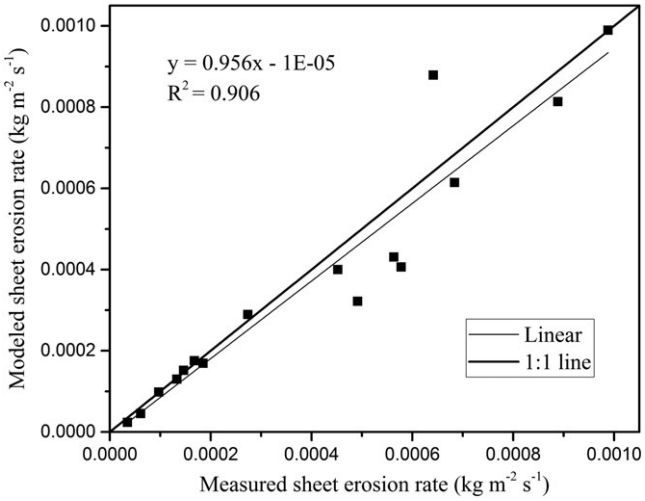

Figure 8. Measured versus modelled sheet erosion rate (SE) (SE=0.0154 (ω–0.00325)).

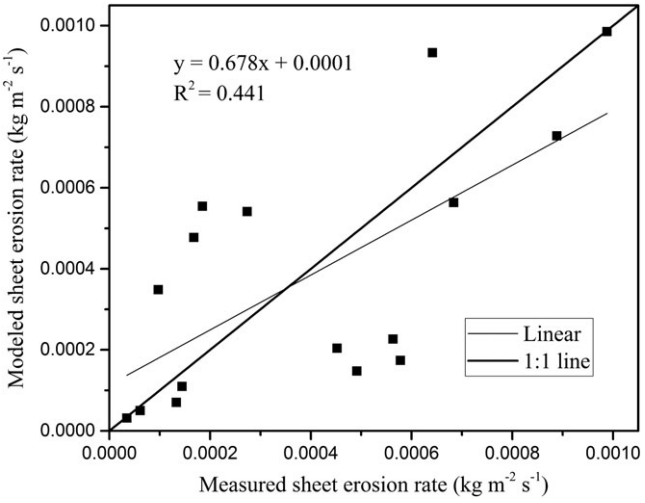

Figure 9. Measured versus modelled sheet erosion rate (SE) (SE=0.0148 (U–0.0003)).

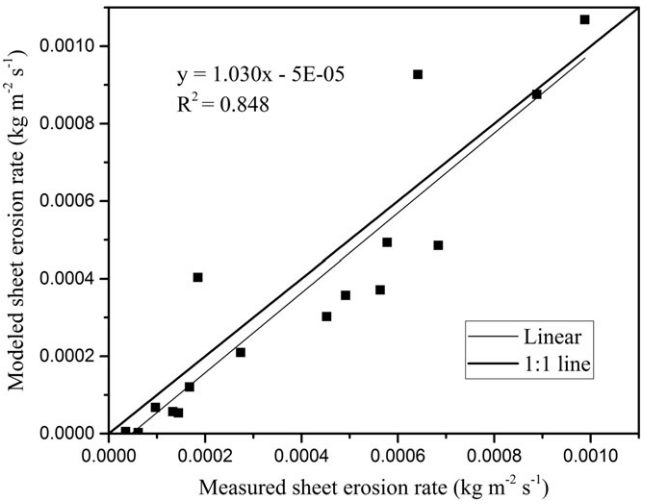

Figure 10. Measured versus modelled sheet erosion rate (SE) (SE = 0.0090 (E – 0.0212)).

Flow shear stress (Equation (1)) is determined by slope and flow depth. Generally, as slope and flow depth increase, flow velocity and mass increase, thereby increasing the kinetic energy of the flow. Therefore, sheet erosion caused by sheet flow increases with flow shear stress. However, flow depth cannot generally increase simultaneously with slope; hence, the coefficient of determination for the relationship between SE caused by sheet flow and shear stress is not very high, indicating that SE is not adequately modelled in this study by a power function equation that includes shear stress (Equation (9)).

Stream power (Equation (2)) is equal to shear stress multiplied by velocity, that is, work divided by time. On the basis of mechanics theory, power is an expression of the rate at which work is done (such as quick or slow), which is a measure of energy change. As stream power increases, the energy loss of flow caused by eroding soil increases; thus, SE as a function of sheet flow increases with stream power. Therefore, the coefficient of determination for the relationship between SE caused by sheet flow and stream power is very high, indicating that SE caused by sheet flow is adequately modelled in this study by a linear equation that includes stream power (Equation (10)).

Unit stream power (Equation (3)) is determined by slope and velocity. As flow velocity and slope increase, flow depth, which implies flow mass, cannot increase simultaneously. Thus, the kinetic energy of flow cannot increase proportionally, and in modelling the sheet erosion caused by sheet flow, the unit stream power is relatively weak. Consequently, the coefficient of determination for the relationship between SE caused by sheet flow and unit stream power is low, which indicates that SE caused by sheet flow is poorly modelled in this study by a linear equation that includes unit stream power (Equation (11)).

Energy is the dynamic source of any movement of matter. In this study, unit energy (Equation (4)) was used to accurately model SE caused by sheet flow. Sheet erosion caused by sheet flow increases with unit energy. Thus, the coefficient of determination for the relationship between SE caused by sheet flow and unit energy is high, which indicates that SE caused by sheet flow is adequately modelled in this study by a linear unit energy equation (Equation (12)). Although energy is the dynamic source of the movement of matter, the rate of energy change (i.e. the rate at which work is done) has a closer relationship with the movement of matter. Consequently, the coefficient of determination for the relationship between SE and stream power is higher than that for unit energy, indicating that SE is better modelled in this study by a linear equation that includes stream power (Equation (11)) than by a linear unit energy equation (Equation (12)).

In addition, the soil erodibility parameter and critical hydraulic parameters in the present study are smaller than those in previous studies (Moore and Burch 1986; Huang 1995; Fan and Wu 1999; Cao *et al*. 2015; Wang *et al*. 2016).

Stream power is the best hydraulic parameter to model SE on rangeland

A comparison of the R^2 and NE values of the response equations of SE to different hydraulic parameters shows that stream power is the best hydraulic parameter for modelling SE. Hence, stream power in this study is suggested for modelling soil erosion, in keeping with recommendations from previous studies (Huang 1995; Moore and Burch, 1986; Cao *et al*. 2015). Stream power is energy-transforming efficiency, which combines velocity and flow depth. Herbaceous vegetation influences both velocity and flow depth. For example, root growth increases the infiltration rate (Morgan *et al*. 1997), grass diameter hinders water flow, and grass blades restrict raindrops (Greene *et al*. 1994) and disturb water flow (Gyssels *et al*. 2005; Durán *et al*. 2006; Durán and Rodríguez, 2008; Baets *et al*. 2007). Therefore, among the four hydraulic parameters, stream power is the best for modelling SE.

A comparison of the modelling result using Equation (10) and that using RHEM (Wei *et al*. 2009; Nearing *et al*. 2011) shows that the equation presented in this study, with NE = 0.89, yielded a better result than that (NE = 0.59) obtained with RHEM when modelling SE under certain conditions.

Improving sheet erosion modelling on rangeland

Measuring velocity on vegetated slopes was difficult in this study. Artificial errors led to several failed experiments. Velocity was calculated when the water flow was straight; however, water does not flow in straight lines on vegetated slopes, which caused the errors. Moreover, velocity was used to calculate hydraulic parameters. Therefore, velocity measurements and calculations should be improved to better quantify modelling result parameters to reflect ecosystem changes (Hernandez *et al*., 2013). Further analysis showed that vegetation has a strong influence on water depth. The value of a bare slope was used to calculate the water depth of the vegetated slope.

Therefore, the formula used to calculate the water depth of vegetated slopes should be modified based on the aggregative indicators of herbaceous vegetation. In the field of statistical analysis, aggregative indicators of herbaceous vegetation for sheet flow should be given greater consideration. In conclusion, velocity measurements and calculations, water depth calculations, and aggregative indicators of herbaceous vegetation for sheet flow should be explored in future research so that sheet erosion can be better modelled.

Using rangeland plot experiments to model SE on rangelands restored from abandoned croplands

The study of SE on rangelands under controlled laboratory conditions is very helpful for revealing the processes and mechanisms. Field conditions, including the coverage, type and distribution of vegetation, slopes, and soil surface features, among other factors, always vary, and rainfall intensities are unsteady. Such field conditions make it difficult to separate the effects of the factors that influence SE, which makes it impossible to reveal the processes and mechanisms of erosion. In this study, we constructed a rangeland plot in the laboratory by filling the plot with soil that had a moisture content and bulk density similar to field values. Grass was transplanted into the soil without disturbing the soil surface, similar to field rangeland conditions. The slope gradient could be adjusted to allow the drainage of infiltrated water from the bottom of the plot. A complementary border area was added around the plot and was filled with soil and transplanted grass in the same manner as the plot to equalize the opportunity for splash both onto and off the plot in an attempt to ensure realistic erosion conditions. This set-up ensured that the conditions in the laboratory resembled those in the field and also guaranteed that the processes and mechanisms of SE could be revealed under controlled laboratory conditions. Numerous steep rangelands have been restored from abandoned steep croplands, and the vegetation coverage on steep rangelands on the Loess Plateau has improved significantly since the Grain-to-Green Project, which restores cropland to forest land or grassland to control soil erosion, was launched in 1999. The restoration period of rangeland vegetation is short ($<$ 20 years); thus, the soil quality restoration period under rangeland vegetation is also short ($<$ 20 years). As steep rangeland was restored from the abandoned steep croplands, the original loess soil of the steep croplands underwent intense erosion, and the soil quality was very poor. Moreover, the soil quality during the short period of restoration lagged behind that of vegetation restoration. Hence, the rangeland plot and the plot soil used in the tests in this study can represent rangeland restored from abandoned croplands and their underlying soil.

Conclusions

The Loess Plateau of China is one of the most severe soil erosion regions in the world. Since the Grain-to-Green Project was launched in 1999, numerous steep rangelands have been restored from abandoned steep croplands, and sheet erosion has become the dominant erosion process on rangelands. Simulated rainfall experiments were performed on rangeland plots, and SE and erosion control on steep rangelands were studied in the loess region.

SE decreases with increasing vegetation cover; this relationship can be well described by linear or logarithmic equations under different rainfall intensities or slopes. Herbaceous vegetation can reduce SE as well as control sheet erosion by decreasing the effect of rainfall intensity or slope, especially under sufficiently high vegetation cover. Moreover, SE can be adequately modelled by a linear equation that includes rainfall intensity, vegetation cover, and slope. Stream power is the best parameter for modelling SE. In addition, velocity measurements and calculations, water depth calculations, and aggregative indicators of herbaceous vegetation for sheet flow are important in improving experimental accuracy and sheet erosion modelling. This study revealed that the quantification of SE and associated dynamics on steep rangelands may aid soil erosion management strategies and improve grassland health.

Acknowledgements—Financial support for this research was provided by the National Key Research and Development Program of China (2016YFC0402401; 2017YFD0800502); the funded project of the National Natural Science Foundation of China (41471230; 41601282; 41171227); Special-Funds of Scientific Research Programs of the State Key Laboratory of Soil Erosion and Dryland Farming on the Loess Plateau (A314021403-C2); and the funded project of the State Key Laboratory of Soil Erosion and Dryland Farming on the Loess Plateau (A314021402-1807).

References

Aradottir AL, Arnalds O. 1985. Gróður á Auðkúlu- og Eyvindarstaðaheiði 1984 og þróun aðferða við ákvörðun á raunverulegu beitarþoli. [Vegetation on Audkuluheidi and Eyvindarstadaheidi commons in 1984, and Methods for Estimating Grazing Capacity. In Icelandic.] Agricultural Research Institute, Reykjavík.

Arnalds O, Thorarinsdottir EF, Metusalemsson S, Jonsson A, Gretarsson G, Arnason A. 2001. *Soil Erosion in Iceland. Soil Conservation Service*: Iceland.

Baets S, Poesen J, Knapen A, Galindo P. 2007. Impact of root architecture on the erosion-reducing potential of roots during concentrated flow. *Earth Surface Processes and Landforms* **32**(9): 1323–1345.

Bagnold RA. 1966. An approach to the sediment transport problem from general physics. *United States Geological Survey Pofessional Paper* **422-i**: 231–291.

Cao L, Zhang K, Dai H, Liang Y. 2015. Modeling interrill erosion on unpaved roads in the loess plateau of China. *Land Degradation Development* **26**(8): 825–832.

Carroll C, Halpin M, Burger P, Bell K, Sallaway MM, Yule DF. 1997. The effect of crop type, crop rotation, and tillage practice on runoff and soil loss on a vertisol in central queensland. *Australian Journal of Soil Research* **35**(4): 925–939.

De Roo APJ, Wesseling CG, Cremers N, *et al*. 1996. LISEM: a physically-based hydrological and soil erosion model incorporated in a GIS [C]. Karel Kovar HP (ed). *Fifth European Conference on Application of Geographic Information Systems in Hydrology and Water Resources Management*, IAHS: Vienna; 1996.

Dlamini P, Orchard C, Jewitt G, Lorentz S, Titshall L, Chaplot V. 2011. Controlling factors of sheet erosion under degraded grasslands in the sloping lands of kwazulu-natal, south Africa. *Agricultural Water Mangement* **98**(11): 1711–1718.

Durán ZVH, Francia MJR, Rodríguez PCR, Martínez RA, Carcéles RB. 2006. Soil-erosion and runoff prevention by plant covers in a mountainous area (SE Spain): implications for sustainable agriculture. *Environmentalist* **26**(4): 309–319.

Durán ZVH, Rodríguez PCR. 2008. Soil-erosion and runoff prevention by plant covers: a review. *Agronomy for Sustainable Development* **28**(1): 65–86.

Fan JC, Wu MF. 1999. Effects of soil strength, texture, slope steepness and rainfall intensity on interrill erosion of some soils in Taiwan. In 10th International Soil Conservation Organization Meeting, Purdue University, USDA-ARS National Soil Erosion Research Laboratory.

Flanagan DC, Nearing MA. 1995. USDA-Water erosion prediction project hillslope profile and watershed model documentation. NSERL Report No. 10, p.1.1-14.28.

Fox DM, Bryan RB. 2000. The relationship of soil loss by interrill erosion to slope gradient. *Catena* **38**(3): 211–222.

Greene RSB, Kinnell PIA, Wood JT. 1994. Role of plant cover and stock trampling on runoff and soil erosion from semi-arid wooded rangelands. *Australian Journal of Soil Research* **32**: 953–973.

Gyssels G, Poesen J, Bochet E, Li Y. 2005. Impact of plant roots on the resistance of soils to erosion by water: a review. *Progress in Physical Geography* **29**(2): 189–217.

Hernandez M, Nearing MA, Stone JJ, Pierson FB, Wei H, Spaeth KE, Weltz MA, Goodrich DC. 2013. Application of a rangeland soil erosion model using National Resources Inventory data in southeastern Arizona. *Journal of Soil & Water Conservation* **68**(6): 512–525.

Horton RE, Leach HR, Van V1iet R. 1934. Laminar sheet flow. *Transactions of the American Geophysical Union* **15**(2): 393–404.

Huang CH. 1995. Empirical analysis of slope and runoff for sediment delivery from interrill areas. *Soil Science Society of America Journal* **59**(4): 982–990.

Liu JE, Wang ZL, Yang XM, Jiao N, Shen N, Ji PF. 2014. The impact of natural polymer derivatives on sheet erosion on experimental loess hillslope. *Soil Tillage Research* **139**: 23–27.

Meyer LD. 1981. How rain intensity affects interrill erosion. *Transactions of ASAE* **24**(6): 1472–1475.

Misra RK, Rose CW. 1996. Application and sensitivity analysis of process-based erosion model GUEST. *European Journal of Soil Science* **47**(4): 593–604.

Moore ID, Burch GJ. 1986. Modelling erosion and deposition. Topographic effects. *Transactions of the ASAE* **29**: 1624–1630.

Morgan RPC. 1995. Soil erosion and conservation. *Geographic Journal* **24**(1): 68–69.

Morgan RPC. 2005. *Soil Erosion and Conservation*. Blackwell Science Ltd.: Oxford.

Morgan RPC, McIntyre K, Vickers AW, Quinton JN, Rickson RJ. 1997. A rainfall simulation study of soil erosion on rangeland in Swaziland. *Soil Tecnil.* **11**: 291–299.

Nash J, Sutcliffe JV. 1970. River flow forecasting through conceptual models part I – A 412 discussion of principles. *Journal of Hydrology* **10**(3): 282–290.

Nearing MA, Bradford JM, Parker SC. 1991. Soil detachment by shallow flow at low slopes. *Soil Science Society of America* **55**(2): 351–357.

Nearing MA, Foster GR, Lane LJ, Finkner SC. 1989. A process-based soil erosion model for usda-water erosion prediction project technology. *Transactions of the ASAE* **32**(5): 1587–1593.

Nearing MA, Wei H, Stone JJ, Pierson FB, Spaeth KE, Weltz MA, Flanagan DC, Hernandez M. 2011. A rangeland hydrology and erosion model. *Transactions of ASABE* **54**: 1–8.

Oudenhoven APEV, Veerkamp CJ, Alkemade R, Leemans R. 2015. Effects of different management regimes on soil erosion and surface runoff in semi-arid to sub-humid rangelands. *Journal of Arid Environments* **120**: 100–111.

Pellant M, Shaver P, Pyke DA, Herrick JE. 2005. Interpreting indicators of rangeland health, version 4. Tech. Ref. 1734–6. BLM/WO/ST00/001 + 1734/REV05. Bureau of Land Managemet, Denver CO.

Prentice IC, Cramer W, Harrison SP, Leemans R, Monserud RA, Solomon AM. 1992. Special paper: a global biome model based on plant physiology and dominance, soil properties and climate. *Journal of Biogeographia* **19**: 117–134.

Prosser IP, Rustomji P. 2000. Sediment transport capacity relations for overland flow. *Programme of Physical Geography* **24**: 179–193.

Pyke DA, Herrick JE, Pellant M. 2002. Rangeland health attributes and indicators for qualitative assessment. *Journal of Range Management* **55**(6): 584–597.

UNEP. 1994. *Environmental Data Report 1993–1994*. United Nations Environmental Programme: Oxford.

Wang DD, Wang ZL, Shen N, Chen H. 2016. Modeling soil detachment capacity by rill flow using hydraulic parameters. *Journal of Hydrology* **535**: 473–479.

Wei H, Nearing MA, Stone JJ. 2007. A comprehensive sensitivity analysis framework for model evaluation and improvement using a case study of the rangeland hydrology and erosion model. *Tranactions of the ASABE* **50**(3): 945–953.

Wei H, Nearing MA, Stone JJ, Breshears DD. 2008. A dual Monte Carlo approach to estimate model uncertainty and its application to the rangeland hydrology and erosion model. *Transactions of the ASABE* **51**(2): 515–520.

Wei H, Nearing MA, Stone JJ, Guertin DP, Spaeth KE, Pierson FB, Nichols MH, Moffett CA. 2009. A new splash and sheet erosion equation for rangelands. *SSSA Journal* **73**(4): 1386–1392.

Wight RJ, Lovely CJ. 1982. Application of soil loss tolerance concept to rangelands. In Proceedings of the Workshop on Estimating Erosion and Sediment Yield on Rangelands, Tucson, AZ. 7–9 March 1981, 199–200. USDA ARM-W-26. USDA-ARS, Oakland, CA.

Williams RE, Allred BE, Denio RM, Paulsen HA. 1968. Conservation, development, and use of the world's rangeland. *Journal of Range Management* **21**: 355–360.

Yang CT. 1972. Unit stream power and sediment transport. *Journal of Hydrology Div-ASCE* **98**: 1805–1826.

Yang CT. 1976. Minimum unit stream power and fluvial hydraulics. *Journal of Hydrology Div-ASCE* **102**: 919–934.

Zhao ZX, He JJ. 2010. *Hydraulics*, 2nd edn; 193–198.

